第32卷第12期 焊 接 学 报 Vol. 32 No. 12
2011年12月 TRANSACTIONS OF THE CHINA WELDING INSTITUTION December 2011

Cu-P基非晶钎料钎焊机理

邹家生， 王 超， 许祥平， 王 磊
(江苏科技大学 先进焊接技术省级重点实验室，镇江 212003)

摘 要： 采用CuP7.7Sn5.4Ni14Si0.2Zr0.04晶态与非晶钎料钎焊紫铜，通过微观手段对比分析了钎焊温度和保温时间对晶态与非晶态钎料钎焊接头成分和组织的影响. 结果表明，CuP7.7Sn5.4Ni14Si0.2Zr0.04非晶钎料钎焊接头由界面区、扩散区以及钎缝中心区组成；随钎焊温度提高或保温时间增加，晶态钎料和非晶钎料钎焊接头界面区和扩散区不断增大，母材热影响区和钎缝中心组织也不断粗化，过高的钎焊温度或过长的保温时间，均会使界面区出现脆性相，但非晶钎料这种影响要小得多；在相同条件下，非晶钎料和母材的相互作用明显比相应的晶态钎料剧烈，其钎缝界面区较为均匀、连续，钎缝中心组织要明显均匀、细小.

关键词： Cu-P基钎料；非晶钎料；微观组织；钎焊机理
中图分类号： TG453 **文献标识码：** A **文章编号：** 0253-360X(2011)12-0033-04

邹家生

0 序 言

传统铜磷钎料的熔点低、流动性好，钎焊温度接近银钎料，且具有自钎性和价格低等优点，是500～800 ℃温度范围内钎焊铜及铜合金取代银基钎料的理想材料[1]. 但Cu-P基钎料由于含有脆性化合物Cu_3P，导致合金在室温下呈脆性，接头强度和韧性比银基钎料差很多，钎料加工困难，用传统方法很难制成箔带，这就导致了Cu-P基钎料应用的局限性[2].

近些年来，采用快速凝固技术制备的非晶型钎料合金，获得了越来越广泛的应用. 非晶箔带钎料成形性好、韧性好、成分均匀，而且解决了传统Cu-P钎料难以成形的问题[3]. 国内部分单位对非晶Cu-P基钎料的成分设计、钎焊工艺等方面的研究取得了一定的进展[4]，然而对于非晶钎料的钎焊机理的研究和报道仍较少. 通过采用CuP7.7Sn 5.4Ni14Si0.2Zr0.04常规与非晶钎料钎焊紫铜，分析对比钎焊温度和钎焊保温时间对晶态与非晶态钎料钎焊接头成分和组织的影响，在此基础上探讨非晶钎料的钎焊机理.

1 试验方法

试验采用的母材为2 mm厚紫铜板，CuP 7.7Sn5.4Ni14Si0.2Zr0.04晶态合金钎料用WK型非自耗真空电弧炉制备，CuP7.7Sn5.4Ni14Si0.2Zr0.04(质量分数，%)非晶合金钎料采用HVDS-II高真空单辊甩带机制备. 采用炉中钎焊的方法对紫铜板搭接接头进行钎焊连接，对钎焊连接后的接头试样用小型试样切割机从钎缝中间切开，制备金相试样，腐蚀剂选用5 g$FeCl_3$ +5 mLHCl +95 mL乙醇溶液. 在ZEISS光学显微镜下观察钎焊接头的微观组织.

收稿日期：2010-09-21
基金项目：江苏省自然科学基金资助项目(BK2007097)

2 试验结果与分析

2.1 CuP7.7Sn5.4Ni14Si0.2Zr0.04非晶合金钎料钎焊接头界面结构

采用CuP7.7Sn5.4Ni14Si0.2Zr0.04非晶合金钎料在温度900 ℃，时间5 min的条件下钎焊紫铜接头微观组织如图1所示. 可以看出钎缝主要由三部分组成：钎缝中心区、界面区以及扩散区. 其中界面区是母材向液态钎料溶入冷却凝固后形成的；而钎缝扩散区则是钎料向固态母材扩散后形成的. 可以发现，钎缝界面区与扩散区为良好的冶金结合，无明显的冶金缺陷，根据前期研究[5]，其结构主要为α-Cu固溶体组成. 钎缝中心区主要由α-Cu固溶体和磷化物脆性相及各种共晶所组成.

2.2 钎焊保温时间对钎焊接头组织的影响

采用CuP7.7Sn5.4Ni14Si0.2Zr0.04晶态钎料与非晶钎料在相同钎焊温度下，钎焊保温时间对钎焊接头组织的影响如图2所示. 图2a，b为保温时

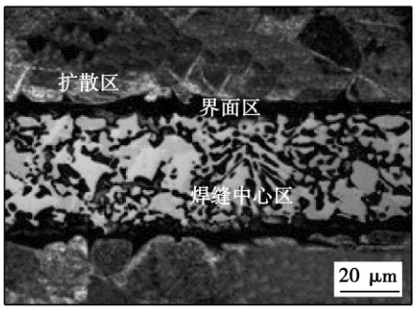

图 1 CuP7.7Sn5.4Ni14Si0.2Zr0.04 非晶钎料钎焊接头组织

Fig. 1 Microstructure of joint brazed with amorphous CuP 7.7Sn5.4Ni14Si0.2Zr0.04 brazing filler metal

间4 min，晶态钎料与非晶钎料钎焊接头的微观组织. 从图 2a，b 可见，由于保温时间短，形成的钎焊接头界面区和扩散区极窄，晶态钎料的界面区还不连续，而非晶钎料在相同条件下，其界面区则较为均匀、连续，说明在相同条件下，非晶钎料和母材的相互作用明显比相应的晶态钎料剧烈；非晶钎料钎焊接头钎缝中心的组织相比晶态钎料，要明显均匀、细小. 对比图 2c ~ 图 2f 均发现了相同的规律，说明在相同条件下，非晶钎料和母材的相互作用剧烈，其钎焊接头的组织比相应的晶态钎料均匀、细小，这从组织角度解释了非晶钎料钎焊接头性能优于晶态钎料的原因. 对比图 2a，c，e，随着钎焊保温时间增加，晶态钎料钎焊接头界面区和扩散区不断增大，母材热影响区和钎缝中心组织也不断粗化. 但仔细分析钎缝中心组织，当钎焊保温时间明显增加时，钎缝中的共晶组织反而减少，原因主要是过长的保温时间导

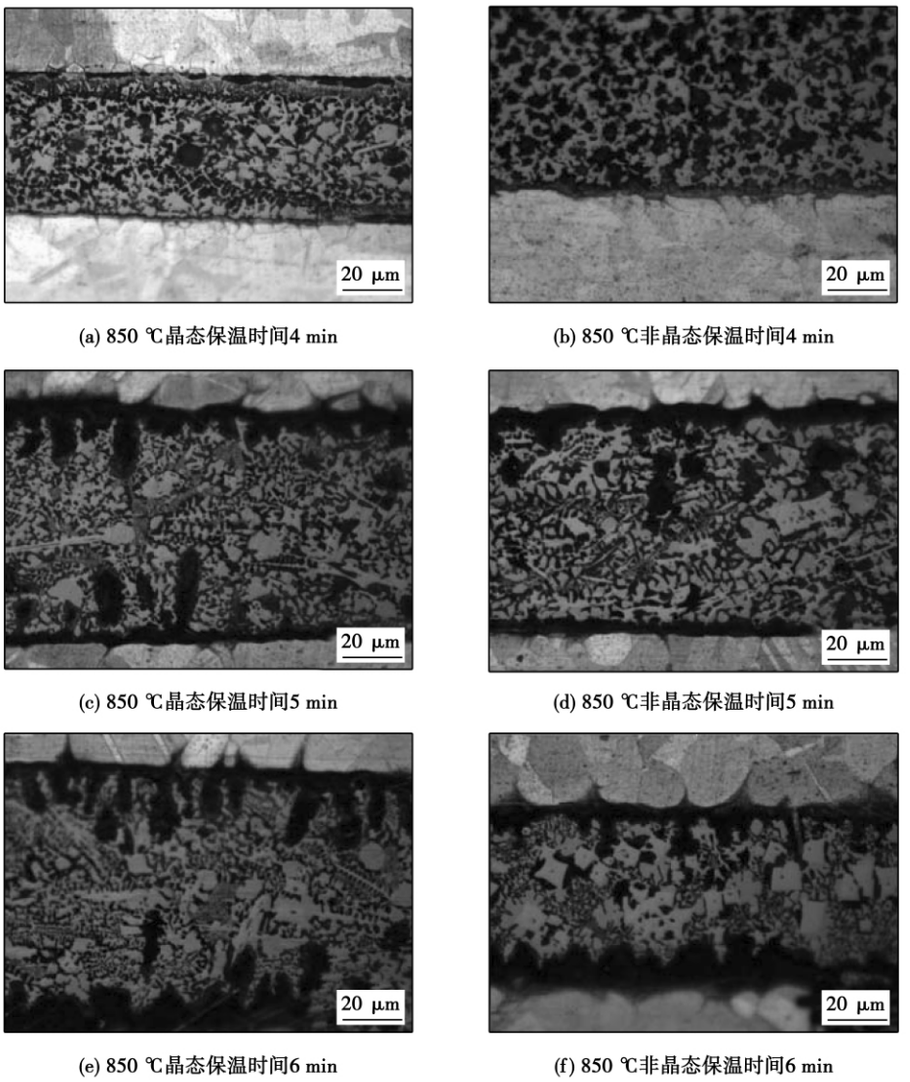

(a) 850 ℃晶态保温时间4 min (b) 850 ℃非晶态保温时间4 min

(c) 850 ℃晶态保温时间5 min (d) 850 ℃非晶态保温时间5 min

(e) 850 ℃晶态保温时间6 min (f) 850 ℃非晶态保温时间6 min

图 2 CuP7.7Sn5.4Ni14Si0.2Zr0.04 晶态和非晶钎料不同保温时间下钎焊接头组织

Fig. 2 Microstructure of CuP7.7Sn5.4Ni14Si0.2Zr0.04 conventional and amorphous brazing seam with different brazing time

致合金元素 P 的烧损所致. 对比图 2b，d，f，发现非晶钎料随着保温时间增加，其接头组织变化亦存在同样的规律.

钎焊时间为 4 min 时，由于钎料和母材作用不充分，界面区与扩散区初形成，合金元素扩散尚未充分进行，故接头强度较低. 随着钎焊时间增加，钎料和母材作用加剧，合金元素扩散充分，界面区与扩散区逐步形成了连续致密的 α-Cu 固溶体层，接头强度提高. 但钎焊时间进一步增加时，由于钎缝和母材晶粒的急剧粗化，而且强偏析合金元素 Sn，P 在界面区的含量超过了其固溶度，界面区中产生了脆性化合物.

2.3　钎焊温度对钎焊接头组织的影响

采用 CuP7.7Sn5.4Ni14Si0.2Zr0.04 晶态钎料与非晶钎料在相同保温时间，不同钎焊温度下晶态钎料与非晶钎料钎焊接头的微观组织如图 3 所示. 从图 3 可见，随钎焊温度提高，母材向液态钎料的溶入和钎料向固态母材的扩散不断加剧造成界面区与扩散区的总厚度不断提高. 钎焊温度为 800 ℃时，此时钎焊接头的界面区和扩散区尚未充分形成，但非晶钎料与晶态钎料相比，其界面区要宽且连续致密，可见其与母材的相互作用明显比相应的晶态钎料剧烈. 在钎缝中心区，晶态钎料的组织较非晶钎料的组织粗大且分布不均. 随钎焊温度升高，界面区和扩散区均增大，钎缝组织粗化. 但从图 3 中发现，随钎焊温度升高，晶态钎料钎焊接头界面区中出现粗大黑色柱状组织，由界面向钎缝中心生长，这可能是钎焊温度升高，合金元素扩散加剧后界面出现的脆性组织，而非晶钎料钎焊接头中这种现象并不明显. 这可能也是相同条件下，非晶钎料钎焊接头

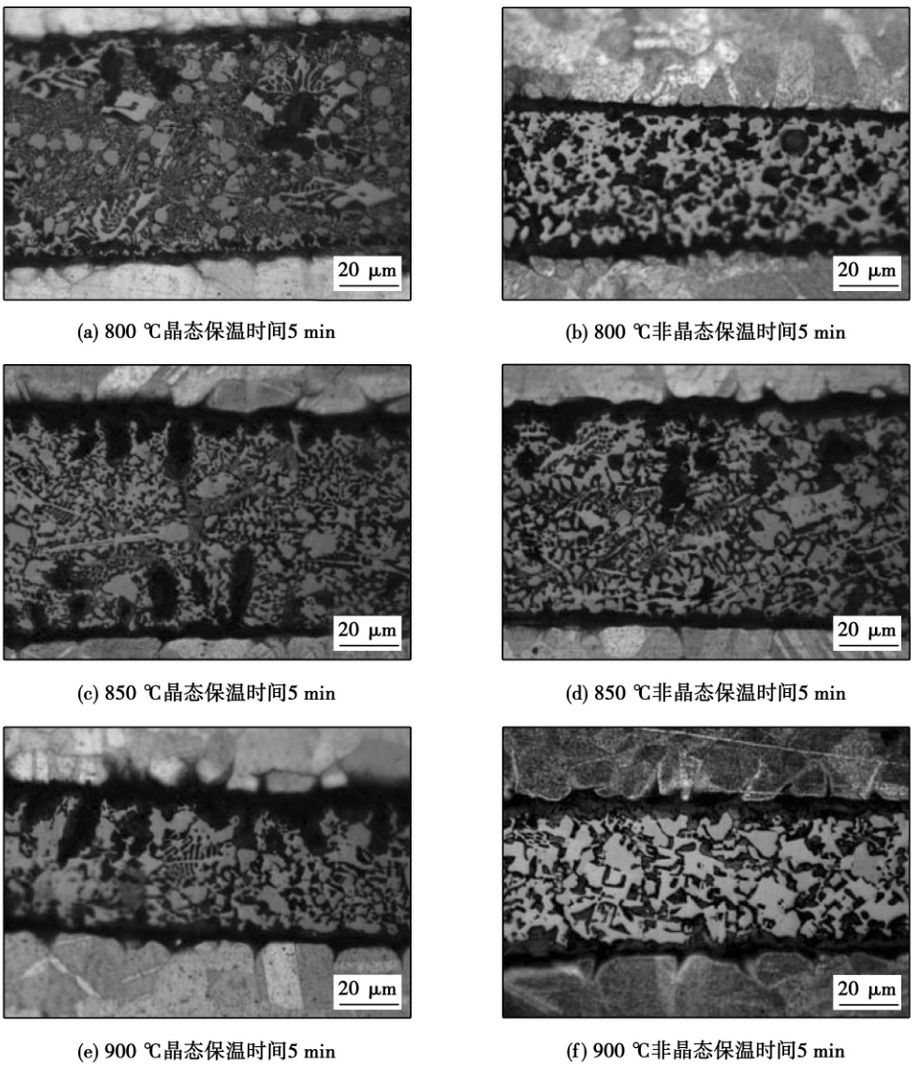

(a) 800 ℃晶态保温时间5 min　(b) 800 ℃非晶态保温时间5 min

(c) 850 ℃晶态保温时间5 min　(d) 850 ℃非晶态保温时间5 min

(e) 900 ℃晶态保温时间5 min　(f) 900 ℃非晶态保温时间5 min

图 3　CuP7.7Sn5.4Ni14Si0.2Zr0.04 晶态和非晶钎料不同温度下钎焊接头的微观组织

Fig. 3　Microstructure of CuP7.7Sn5.4Ni14Si0.2Zr0.04 conventional and amorphous brazing seam with different brazing temperature

性能高于晶态钎料的原因之一.

钎焊温度为800 ℃时,由于温度较低,液态钎料和母材的相互作用还不够充分,因此形成的界面区与扩散区均较窄,接头强度也较低. 当钎焊温度为850 ℃时,界面区与扩散区增大,合金元素P,Sn向母材扩散加剧,降低了界面区中磷、锡含量,使界面区结构主要由连续致密的α-Cu固溶体组成,避免出现脆性的磷、锡化合物相. 但钎焊温度进一步升高,界面区与扩散区继续增大,钎缝中心合金元素P,Sn向界面区与扩散区的扩散加剧,使界面区中磷、锡含量反而升高,甚至超过其固溶度,出现脆性相,使接头性能降低. 当然,过高的钎焊温度使钎缝和母材组织晶粒粗化亦使接头力学性能降低.

3 结 论

(1) CuP7.7Sn5.4Ni14Si0.2Zr0.04非晶钎料钎焊接头由界面区、扩散区及钎缝中心区组成,扩散区和界面区主要是α-Cu固溶体组成,钎缝中心区主要由α-Cu固溶体和磷化物脆性相及各种共晶组成.

(2) 随钎焊温度提高或保温时间增加,晶态钎料和非晶钎料钎焊接头界面区和扩散区不断增大,母材热影响区和钎缝中心组织也不断粗化. 但过高的钎焊温度或过长的保温时间,均会使界面区出现脆性相,但非晶钎料这种影响要小得多. 在相同条件下,非晶钎料和母材的相互作用明显比相应的晶态钎料剧烈,其钎缝界面区较为均匀、连续,钎缝中心组织要明显均匀、细小.

参考文献:

[1] 李宝锦,李英龙. 磷铜钎料的研究与应用[J]. 黄金学报,1999,1(2):151-153.
Li Baojin, Li Yinglong. Phosphor copper brazing filler metals research and application[J]. Journal of Gold, 1999, 1(2): 151-153.

[2] 韩逸生,邹家生,陈 铮,等. Ag-P-Cu钎料中Ag的作用分析[J]. 焊接技术,2000,29(3):23-24.
Han Yisheng, Zou Jiasheng, Chen Zheng, *et al*. Ag-P-Cu behavior in the Ag brazing filler metals[J]. Welding Technique, 2000, 29(3): 23-24.

[3] 李 刚,路文江,俞伟元,等. 非晶新型带银钎料的制备及性能研究[J]. 兰州理工大学学报,2004,30(5):9-12.
Li Gang, Lu Wenjiang, Yu Weiyuan, *et al*. Amorphous new take the synthesis and properties of silver brazing filler metals[J]. Journal of Lanzhou University, 2004, 30(5): 9-12.

[4] Zou Jiasheng, Xu Zhirong, Jiang Zhiguo. Study on Ti-based amorphous brazing alloy[J]. Transactions of Nonferrous Metals Society of China, 2006, 16(2): 171-174.

[5] 蒋志国,邹家生. Ti-Zr-Ni-Cu非晶钎料钎焊Si_3N_4陶瓷的连接强度[J]. 中国有色金属学报,2006,16(11):1955-1959.
Jiang Zhiguo, Zou Jiasheng. Ti-Zr-Ni-Cu amorphous Si_3N_4 ceramics analyzed brazing[J]. Connection Strength of China Nonferrous Metals, 2006, 16(11): 1955-1959.

作者简介: 邹家生,男,1965年出生,教授,博士. 主要研究方向为新材料及其连接技术. 发表论文90余篇. Email: zjzoujs@126.com

[上接第4页]

表征量[J]. 焊接学报,2006,27(3):1-4.
Wu Qingsheng, He Jingshan, Feng Jicai. Characterization parameter of aluminum alloy weld appearance of electron beam welding[J]. Transactions of the China Welding Institution, 2006, 27(3): 1-4.

[2] Li Yunfeng, Zhao Xihua, Li Yongqiang. Vision-based detection of weld pool width in TIG welding of copper-clad aluminum cable[J]. China Welding, 2007, 16(3): 27-31.

[3] Rafer C Gonzalez, Richard E Woods. digital image processing second edition[M]. Beijing: Publishing House of Electronics Industry, 2002.

[4] 戴青云,余英林. 数学形态学在图象处理中的应用进展[J]. 控制理论与应用,2001,18(4):478-482.
Dai Qingyun, Yu Yinglin. The advances of mathematical morphology in image processing[J]. Control Theory and Applicatiions, 2001, 18(4): 478-482.

[5] 贺兴华. MATLAB7.X图像处理[M]. 北京:人民邮电出版社,2006.

[6] 刘明涛,高向东,陈建辉,等. 基于数学形态学的熔池图像处理[J]. 焊接,2008(5):29-32.
Liu Mingtao, Gao Xiangdong, Chen Jianhui, *et al*. Processing on molten pool image based on morphology[J]. Welding & Joining, 2008(5): 29-32.

[7] 何晓群. 现代统计分析方法与应用[M]. 北京:中国人民大学出版社,1998.

[8] 蔡 艳,杨海澜,徐 忻,等. 基于偏最小二乘回归方法的CO_2焊飞溅模型[J]. 焊接学报,2004,25(5):125-128.
Cai Yan, Yang Hailan, Xu Xin, *et al*. Spatter model of CO_2 welding based on partial least squares regression method[J]. Transactions of the China Welding Institution, 2004, 25(5): 125-128.

[9] 滕素珍,姜炳蔚,任玉杰,等. 数理统计[M]. 2版. 大连:大连理工大学出版社,1996.

作者简介: 张秉刚,男,1971年出生,博士,副教授. 研究方向为新材料及异种材料电子束焊接. 已发表论文40余篇. Email: zhangbg@hit.edu.cn

通讯作者: 石铭霄,男,1982年出生,博士. Email: hero-4587@163.com

chine DU Suigeng, YANG Zhengqiang, YU Longqi (Key Laboratory of Ministry of Education for Contemporary Design and Integrated Manufacturing Technology, Northwestern Polytechnical University, Xi´an 710072, China). p 17 - 20

Abstract: In view of the issues that the control effect of the load system of friction welding machine on pressure mutation phases is unsatisfactory with (proportion integration) closed-loop control algorithm, the fuzzy PI control algorithm is introduced. According to the error and its changing trend of the actual value and the set value, the whole control process is divided into four kinds of control intervals. Based on optimizing the fuzzy control degree, the corresponding fuzzy rules and parameters determining methods are developed. Under the test conditions, the control effects of four control intervals with the different control parameters are contrasted, the best fit coefficients of every control interval are obtained. The performance indicators using fuzzy PI control methods are better than that using traditional PI control methods. Under test conditions with the optimizing fuzzy control degree and the best fit coefficients, the maximum overshoot has been reduced 19.2%, the adjust time has been reduced 1.59 s, and the steady precision has been raised 0.4%.

Key words: friction welding machine; computer control; fuzzy-PI; control algorithm

Effect of laser on pulsed MAG arc radiation LIU Deshen[1], LI Huan[1], WANG Xuyou[2], WANG Wei[2], GAO Ying[3] (1. Tianjin Key Laboratory of Advanced Joining Technology, Tianjin University, Tianjin 300072, China; 2. Harbin Welding Institute, Harbin 150080, China; 3. Tianjin Key Laboratory of High Speed Cutting and Precision Machining, Tianjin University of Technology and Education, Tianjin 300222, China). p 21 - 24

Abstract: The laser-pulsed MAG hybrid welding system and acquisition system were set up to get the electric signal and arc spectrum under the conditions with and without laser. To analyze the relationship between arc energy input and the spectral radiation intensity of FeII274.648, FeI382.043, FeI492.050 and ArI801.479 using the method of linear fit. Studies have shown that the spectral radiation intensity of the four feature spectrum lines are proportion to arc energy input. With the same arc energy input, the arc radiation intensity of hybrid welding is smaller than the one of pulsed MAG welding. This is because the metal vapor and plasma produced by laser may absorb the arc plasma radiation.

Key words: laser hybrid welding; energy input; radiation intensity; linear fit

Microstructure of solder joints with micron stand-off height in electronic packaging WANG Bo[1,2], MO Liping[1], WU Fengshun[1,2], XIA Weisheng[1], WU Yiping[1,2] (1. State Key Laboratory of Material Processing and Die & Mould Technology, Huazhong University of Science and Technology, Wuhan 430074, China; 2. Wuhan National Laboratory for Optoelectronics, Wuhan 430074, China). p 25 - 28

Abstract: In present paper the microstructural change was studied when the stand-off height (SOH) of solder joints with Cu/Sn/Cu sandwich structure was reduced from 100 μm to 50 μm, 20 μm and 10 μm. With the reducing stand-off height, the Cu content increases in the solder bulk, and the Cu_6Sn_5 intermetallic layer formed at both sides decreases in thickness; while the proportion of IMC thickness to solder joint stand-off height increases. The thickness of the copper layer consumed by solder joints with different stand-off heights was calculated according to the formed IMC layer and Cu content in the solder bulk. It is found that the consumed copper thickness decreases with the reducing stand-off height. In the aging, the solder joint with lower SOH increases faster in IMC thickness and IMC proportion, leading to more dramatic microstructural change.

Key words: electronic packaging solder joint; stand-off height; micro structure

Morphologies and growth mechanism of TiN in ceramic surface layers prepared by nitrogen arc ZHENG Xiaoyi[1], CONG Dazhi[2], LI Xin[1], ZHAO Lei[1], LI Yuhua[1], REN Zhenan[1] (1. College of Materials Science and Engineering, Jilin University, Changchun 130022, China; 2. Shanghai Nuclear Engineering Research & Design Institute, Shanghai 200233, China). p 29 - 32

Abstract: The titanium nitride (TiN) ceramic surface layers were in-situ prepared by nitrogen arc melting on the surface of pure titanium substrates. The formation mechanism of the ceramic layers, the growth morphologies and mechanism of the TiN phase were investigated. The results show that the nitrogen arc melting is a non-equilibrium rapid cooling process and the cooling rate can be as high as $10^2 \sim 10^3$ K/s. The micro growth modes of the TiN phase in ceramic surface layers exhibit the diversity. The TiN crystal grows up by the spiral dislocation lateral growth mode at the location of low undercooling in the molten pool. Because of the undercooling increased at the bottom of the molten pool, the micro growth mode changes to the alternating between the continuous growth and the lateral growth.

Key words: nitrogen arc; titanium nitride; morphology; growth mechanism

Bonding mechanism of brazing of amorphous Cu-P filler metal ZOU Jiasheng, WANG Chao, XU Xiangping, WANG Lei (Provincial Key Lab of Advanced Welding Technology, Jiangsu University of Science and Technology, Zhenjiang 212003, China). p 33 - 36

Abstract: The copper joints were brazed with CuP 7.7 Sn5.4Ni14Si0.2Zr0.04 amorphous filler metal conventional filler metal respectively. The effect of the brazing temperature and time on the crystalline composition and microstructure of joints brazed with the amorphous brazing filler metal were compared and analyzed by micro-method. The results showed that the joints brazed with CuP7.7Sn5.4Ni14Si0.2Zr0.04 amorphous brazing filler metal consist of centre zone, interface area and diffusion zone. With the increase of brazing temperature and brazing holding time, the interface area brazed with both amorphous and conventional filler metal increases, and the microstructures of base metal and brazinrg seam centre zone would be coarsed. Excessively high brazing temperature or long brazing holding time will produce brittle phase, but this effect on amorphous filler metals is much smaller. Under the same conditions, amorphous filler metals interact with the base metal much more intensely than the corresponding conventional filler metals. The microstructure in interface area and centre zone of amorphous brazing seam are evidently uniform and small.

Key words: Cu-P based filler metal; amorphous filler

metal; microstructure; brazing mechanism

Interfacial characteristics of welded joint between aluminum alloy and stainless steel by resistance spot welding QIU Ranfeng[1,2], YU Hua[1], SHI Hongxin[1], ZHAN Keke[1], TU Yimin[1], SATONAKA Shinobu[3] (1. School of Materials Science and Engineering, Henan University of Science and Technology, Luoyang 471003, China; 2. Henan Key Laboratory of Advanced Non-ferrous Metals, Luoyang 471003, China; 3. Graduate School of Science and Technology, Kumamoto University, Kurokami 2-39-1, Kumamoto 860-8555, Japan). p 37 - 40

Abstract: Aluminum alloy A5052 and stainless steel SUS304 were welded by resistance spot welding with a cover plate. The welding interface region of the joint was observed with electron microscopy, and the microstructure and distribution of the reaction products were analyzed as well. The results reveal that a serration reaction layer consisting of Fe_2Al_5 and $FeAl_3$ forms in the welding interface and the reaction layer thickness varies with the welding current and the position at the welding interface. Moreover, the reaction blocks in aluminum alloy near the welding interface were observed, which were estimated as a hexagonal AlFeCr having $a = 2.451$ nm and $c = 0.758$ nm based on analysis of selected area electron diffraction patterns.

Key words: aluminum alloy; stainless steel; resistance spot welding; interface reaction layer

Study on cold metal transfer welded lap joints of Mg/Al dissimilar metals SHANG Jing[1], WANG Kehong[1], TIAN Hongjun[2], ZHOU Qi[1], LI Guangle[1] (1. School of Material Science and Engineering, Nanjing University of Science and Technology, Nanjing 210094, China; 2. State-owned 5103 Factory, Nanzhao 474650, China). p 41 - 45

Abstract: AZ31B magnesium alloy and 6061 aluminum alloy were welded by cold metal transfer (CMT) welding method with pure copper (HS201) as the filler metal. Shear strength and micro-hardness of the lap joint were tested. The microstructure and fracture morphology of joint were studied by means of scanning electron microscope (SEM) and energy dispersive X-ray (EDX). The results showed that good weld with the highest shear bonding strength of 27.9MPa was obtained under the welding current of 109 A, welding voltage of 10.9 V, wire feed speed of 4.9 mm/s, welding speed of 0.45 m/min. Intermetallic compounds of Mg_2Cu and $MgCu_2$ were formed in the Mg-Cu side where was oxidized. Al-Cu-Mg ternary intermetallic compounds and Al_2Cu were formed on the Al-Cu side. Micro-hardness in both sides of fusion zone was suddenly increased due to intermetallic compounds. Maximum micro-hardness of Al-Cu side and Mg-Cu side were 242 HV and 347 HV respectively. The fracture occurred in the fusion zone of Mg side, and fracture nature was brittle fracture. Oxidation in the welding process and plenty of intermetallic compounds distributed continuously in the fusion zone, and resulted in the fracture.

Key words: cold metal transfer welding; aluminum alloy; magnesium alloy; dissimilar metals welding; intermetallic compounds

Preparation and properties of composite ceramic coating on AZ31B alloy by thermo-chemical reaction spraying MA Zhuang, ZOU Jifeng, WANG Wei, LI Zhichao (Institute of Materials Processing and Surface Technology, Liaoning Technical University, Fuxin 123000, China). p 46 - 50

Abstract: The spraying composite powder was prepared by mechanical ball milling and polyvinyl alcohol (PVA) granulation. Al_2O_3-based composite ceramic coating was prepared on the surface of magnesium alloy AZ31B by thermo-chemical reaction spraying. XRD and SEM were used to analyze the composition and morphology of the spraying composite powder and composite ceramic coating. The thermal shock, compactness, microhardness and wear properties of the composite ceramic coating were investigated respectively. The results showed that chemical reaction had happened in composite powder after 12 hours ball milling and globular structure coated each other was formed after granulation. Thermo-chemical reaction was carried out in the process of preparing coatings. New phase such as $Al_{3.21}Si_{0.47}$, $MgAl_2O_4$ and $Mg_{3.5}Al_9Si_{1.5}O_{20}$ were found in the coating. The melting rate of composite ceramic coating was high and the combination of the coating and matrix was good. Mg element took place remarkable diffusion in the interface of composite coating. The thermal-shock times of this coating was 40, the porosity was 15.1% and the maximum microhardness value reached $HV_{0.1}$ 1016. The thermal shock, compactness, microhardness and wear properties of this coating was significantly better than the ones with common spraying coating.

Key words: magnesium alloy; thermo-chemical reaction spraying; ceramic coating; performance

Influence of gas shroud on property of plasma sprayed thermal barrier coating WEI Qi, LI Hui, LI Hong, ZHANG Linwei (College of Materials Science and Engineering, Beijing University of Technology, Beijing 100124, China). p 51 - 54

Abstract: The comparative study were carried out on the microstructure as well as the properties of the coating prepared by atmospheric plasma spraying and shroud plasma spraying. The results showed that, compared to the conventional atmospheric plasma sprayed (APS) coating, the shroud plasma sprayed (SPS) coating contained less unmelted or partially melted particles and oxide content, and porosity was lower. The SPS coating presented superior oxidation resistance at 1 080 ℃ than the APS one. The reason owed to the mitigation of the involvement of the surrounding air that caused turbulent of the plasma, consequently, the particles were more fully melted and less oxide formed in the coating. The finally deposited SPS coating was denser and contained more Al element, which induced the formation of compact Al_2O_3 layer at the early stage of oxidation. This compact Al_2O_3 layer would slow down the thickening rate of thermally grown oxide (TGO) that provides better resistance to the bond layer, therefore the SPS coating presents higher resistance to high temperature oxidation.

Key words: plasma spray; thermal barrier coating; oxidation resistance

Influence of welding sequence on welding residual stress distribution in thick plate joint DENG Dean[1], SHOICHI Kiyoshima[2] (1. College of Materials Science and Engineering, Chongqing University, Chongqing 400045, China; 2. Research Center of Computational Mechanics, Inc., Tokyo 142-0041, Japan). p 55 - 58

Abstract: Features of welding residual stress distribution in an austenitic stainless steel thick plate joint were investigated by means of experiment and numerical simulation technology.